IEEE Access
Multidisciplinary ⋮ Rapid Review ⋮ Open Access Journal

Received July 3, 2018, accepted July 29, 2018, date of publication August 1, 2018, date of current version August 20, 2018.

*Digital Object Identifier 10.1109/ACCESS.2018.2861940*

# Visual Search Efficiency Evaluation Method for Potential Connected Vehicles on Sharp Curves

**JINSHUAN PENG, CHENWEI WANG, YIMING SHAO, AND JIN XU**
Chongqing Key Laboratory of Transportation Engineering, Chongqing Jiaotong University, Chongqing 400074, China

Corresponding author: Jinshuan Peng (pengjinshuan@163.com)

This work was supported in part by the National Natural Science Foundation of China under Grant 61503049, in part by the China Postdoctoral Science Foundation Funded Project under Grant 2016T90838 and Grant 2015M582525, in part by the Special Funding Project for Research Projects of Postdoctoral Researchers in Chongqing under Grant Xm2016056, in part by the Specialized Research Fund for the Doctoral Program of Higher Education of China under Grant 20135522110003, and in part by the Open Fund of Chongqing Key Laboratory of Traffic&Transportation under Grant 2016CQJY004.

**ABSTRACT** Accurate discrimination of driving proficiency is essential to improve driving safety. A naturalistic driving experiment was designed and organized to discover the response characteristics among drivers' eye movement behaviors, driving proficiency, and mountain roads; 20 drivers were recruited to collect corresponding data of eye movement parameters on sharp turns, including gaze behavior and saccade behavior. The data show that on right turning roads, the main range of eye fixation points is −0.1–0.3 m in the horizontal direction, while the range is −0.35–0.2 m for left turn bends. The main range of the eye horizontal gaze angle is 0–30°, the range of the saccade amplitude is 5–25°, and its value increased as the curve radius decreased, showing a logarithmic relationship. Based on the collected eye movement characteristics data, a driver's visual search modal matrix was built. A principal component analysis was used, and a comprehensive evaluation model of drivers' eye movement characteristics was established. The result shows that eye movement comprehensive score and driving mileage were positively correlated. The result also indicates that the discrimination model can be used to quantify and discriminate driving proficiency and can provide a novel perspective for connected vehicle performance assessment.

**INDEX TERMS** Internet of Things, driving behavior, eye movement characteristics, mountain road, principal component analysis, driving proficiency.

## I. INTRODUCTION

It is well-known that car driving proficiency level is a general evaluation of driving skills, which can reflect driving experience to a certain extent in vehicle operation and road information acquisition or processing. The data show that many traffic accidents are caused by the driver's unskilled operation [1], [2]. In 2015, drivers in China with less than three years of driving experience caused 14854 deaths, accounting for 25.6% of deaths in this year [3]. Furthermore, there were 6 major and more severe accidents on bended roads, accounting for 50% of deaths [4]. Driving proficiency assessment and high-level driving skill driver-selection can reduce potential casualties and property losses.

To assess the operational proficiency of drivers, many scholars and researchers at home and abroad mainly have used driving self-reports and simulated driving. The positive correlation between perceived practical driver competence and self-assessment of driving skills indicates that actual driving ability can be analyzed by constructing a self-assessment system for perceived driving ability [5]–[8]. Situational awareness has been assessed by natural driving video analysis methods and by different driver perceptions of traffic scenarios. It was found that older drivers matched and often exceeded younger drivers when their SA scores were compared individually. However, younger drivers out-performed their older counterparts in hazard perception ability, and this was shown to be related to their situational awareness score [9]–[11]. The differences in visual search characteristics between skilled and unskilled drivers have been tested on different types of roads [12], [13]. Comparing drivers' performances in a driving simulator as well as the self-assessment of specific driving skills, it was found that self-assessments were inconsistent with the driving performance, especially in terms of risk prediction and judgment [14], [15].

In natural driving, the road conditions and the surrounding environment are the main factors for drivers to obtain driving information, and more than 80% of this kind of information needs to be obtained through drivers' eyes [16]. Therefore, visual feature extraction is an important means to analyze driving behaviors. The change of eye movements in the course of unskilled to skilled driving has shown that skilled drivers pay more attention to road information and recognize more complex information [17]–[19]. Zhang used an actual road test to study the relationship between eye movement velocity and the road line shape and found a significant linear correlation between the changing rate of eye movement velocity and the curve radius, as well as the longitudinal slope of the road [20]. In addition, when driving along a sharp bend of a mountain road (the radius of a bend is less than 50 m), the driving horizon is seriously inadequate, the level of traffic safety facilities is low, and traffic accidents easily happen; thus, higher visual searching requirements are put forth [21], [22].

The above analysis shows that there are profound differences in visual search rules among drivers of different driving styles; however, currently, there are few achievements in synthetically considering the characteristics of visual search and mountain road alignment parameters. Based on an analysis of drivers' visual search characteristics, a naturalistic driving behavior experiment is organized to explore an evaluation method of drivers' eye movement characteristics and driving proficiency on the sharp bend section of a mountain road. This method contributes to selecting, evaluating and training drivers in transportation enterprises, and providing the parameter design demand of autonomous vehicles under complex sharp curve conditions. Therefore, reduces risks of road traffic systems from a human perspective and improves traffic safety levels.

## II. EXPERIMENT

### A. TEST ROAD

The provincial road of S103 Nanxi to Hongtu section in Chongqing, China, was selected as the test road. This road section is 60 km, is two lanes (two-way), has a speed limit of 50 km/h, and is separated by a central line. The experimental section is a complex mountain road with 114 typical bends, of which 24 are sharp bends. Before the test, by contacting the traffic police and related design departments, many important road parameters are obtained, such as the slope of the test section, the radius of circle curves, the curvature of clothoid curves, and the horizontal and vertical line parameters (circular curve radius and the curve angle). Combined with road design data, the starting and ending points of the sharp curves are marked in advance, which is convenient for recording the test data.

### B. SUBJECTS

Twenty test drivers were recruited to conduct the experiments, who meet the following conditions: more than two years of driving experience, at least 50,000 kilometers of driving mileage, and no visual, physical, or psychological impairments. Finally, 16 male drivers and 4 female drivers were selected (Table 2). The subjects were between the ages of 26 and 48, with an average age of 37.25 years and a standard deviation of 5.82 years. After completing the experiment, the subjects were reimbursed for a certain amount of their lost income.

### C. TEST METHOD

To collect data on eye movement characteristics, an integrated data collection platform was developed, including the following sensors and devices: Toyota Sea Lion 9-seater commercial bus, Smart Eye Pro5.7 non-contact visual tracker (for detecting eye movement characteristics, such as fixation point distribution, horizontal or vertical gaze angle, saccade duration, etc.), VBOX (for recording vehicle velocities, lateral accelerations, longitudinal accelerations, yaw rates, etc.), a data acquisition meter, a physiological status acquisition meter and a driving recorder. In addition, the non-contact visual tracker enables drivers to drive a vehicle in a natural state, which means that the visual search characteristics are not disturbed by the equipment installed on the car and that more accurate and effective visual data are collected. Thus, it is much easier to analyze the difference in dynamic visual search characteristics of drivers with different driving proficiencies. At the same time, the tracker can also overcome the loss of sight tracking caused by severe head movement. Figure 1 shows the test vehicle, the associated equipment and the test scene.

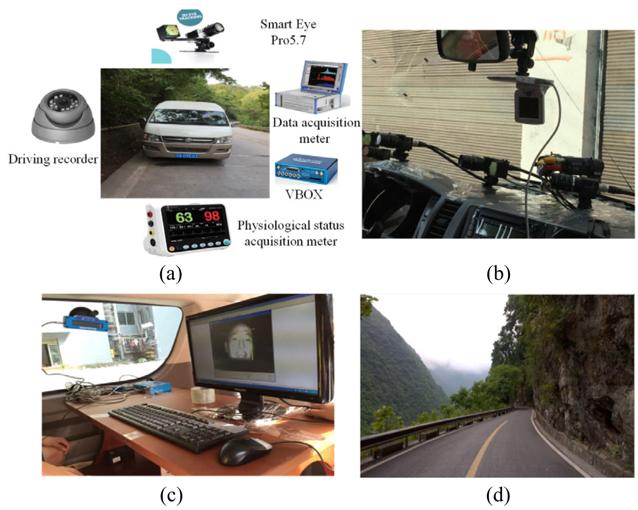


**FIGURE 1.** Experimental design. (a) Majar devices. (b) Installed position. (c) Data collecting platform. (d) Test road.

After installation of the relevant basic devices, a pre-test is required to ensure that devices run normally during driving processes. The test should be carried out in good weather conditions and in an appropriate period. Inquiries and heart rate measurements are required before each driving session starts, which enable drivers to complete the experiment in good psychological and physiological conditions. At the end of each test, it is necessary to re-calibrate the devices to avoid data errors caused by uneven roads or other environmental factors.

## III. VISUAL SEARCH PARAMETER ANALYSIS

During the process of a car passing through bends, the test devices can be used to directly collect eye movement characteristic data, including fixation point positions, horizontal gaze angles, vertical gaze angles, scanning durations and saccade amplitudes. In addition, other indicators can be obtained through mathematical calculation with the above indexes, such as saccade velocity. The schematic diagram in Figure 2 is used to illustrate the definition of the visual representation parameters.

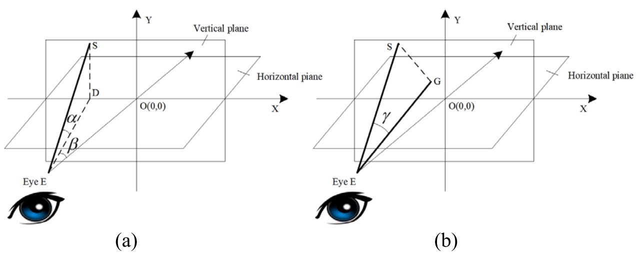


**FIGURE 2. Schematic of the visual parameters. (a) Gaze behavior. (b) Saccade behavior.**

$E$ is the position of the driver's eyes, the origin $O(0, 0)$ indicates the intersection point between the perpendicular line of the driver's eye to a fixed vertical plane and the horizontal plane. Picture a) is mainly used to explain drivers' gaze behavior, and b) is used to explain drivers' saccade behavior. In picture a), the intersection point between the drivers' line of sight and the vertical plane is recorded as the driver's fixation point position $S$. From the fixation point $S$ to the X axis, a vertical line is made at point $D$. Then, by connecting eye position $E$ and foot $D$, the angle $\angle SED$ between the line of sight and line $DE$ is obtained, which is the eye vertical gaze angle, recorded as $\alpha$. The angle $\angle DEO$ between the line of sight and the vertical plane is obtained, which is the eye horizontal gaze angle, recorded as $\beta$. In picture b), the first fixation point position is noted as $S$, and the second position is $G$. The angle $\angle SEG$ between these lines of sight is the driver's visual saccade amplitude, denoted as $\gamma$.

### A. FIXATION POINT POSITION

The fixation point location is the spatial focus of the driver's sight for a period of time. The length of time that a fixation point stays in a certain vision field can reflect the eye fixation area in a driver's driving process [23], [24]. The eye fixation point position is an index to measure the visual search efficiency, representing the attention area or object in a driver's visual search field range under certain conditions. The more focused gaze areas indicate that the information density in this area is higher, and the driver's attention to the area is also higher. Figure 3 shows the fixation point location of all 20 drivers for all sharp bends. The horizontal and vertical axes represent the horizontal and vertical displacements of the fixation point, respectively. The origin of the fixation was the projection of the line of sight onto the forward vertical plane in a normal driver sitting position.

Area of the covered rectangular zone (ACRZ) for the fixation points was defined to represent their dispersion degree. From the above figure, for the sharp right turn bends, the distribution range of horizontal eye gaze points is −0.1-0.25 m, and the main range in the vertical direction is −0.06-0.16 m ($ACRZ_1 = 0.077\ m^2$), which indicates that eye sight is more concentrated on the area above the horizontal surface and to the right of the vertical surface. For the left sharp turn bends, the distribution range of the eye fixation points is −0.35-0.18 m in the horizontal direction, and the main range in the vertical direction is −0.08-0.18 m ($ACRZ_2 = 0.1387\ m^2$), indicating that the driver's sight is more concentrated on the area above the horizontal surface and to the left of the vertical surface. When drivers pass through sharp bends, therefore, eye sight mainly focuses on inside and front road information.

The curve radius and direction were considered independent variables to analyze the characteristics of the fixation point distribution of drivers on a curved road section. The following four typical curved road sections were selected: right turn, curve radius 45.2 m; right turn, curve radius 150.7 m; left turn, curve radius 33.5 m; and left turn, curve radius 135.7 m. Fixation points from all the participants through the above curved road sections were superimposed and quantified, and the results are shown in Figure 4.

When turning right, the horizontal displacement of the fixation points was -0.1 to 0.3 m, and the vertical displacement was -0.05 to 0.18 m. Comparing Figures 4a) and 4b), it can be seen that the larger the curve radius, the more diffuse the fixation point distribution ($ACRZ_3 = 0.057\ m^2$, $ACRZ_4 = 0.0884\ m^2$), which indicates that the driver is in a relatively comfortable driving state. As the curve radius decreases, the effective stopping sight distance of the curve decreases. To effectively guarantee driving safety, drivers will focus more visual attention on targets on the inside of the curve, such as road markings and guardrails as well as the right side of the mountain. When turning right, with a small curve radius, the fixation points of drivers are more displaced towards the right.

When turning left, the horizontal displacement of the fixation points was −0.35 to 0.21 m, and the vertical displacement was −0.07 to 0.24 m. Similar to the right turn, the larger the curve radius, the more diffuse the fixation point distribution ($ACRZ_5 = 0.1225\ m^2$, $ACRZ_6 = 0.1728\ m^2$); with a small curve radius, the fixation points of drivers are more displaced towards the left. As the curve radius increases, the effective stopping sight distance of the curve increases correspondingly, and drivers are in a more relaxed driving state. To effectively guarantee roadside driving safety, when turning left in curves with a large radius, drivers will focus more visual attention on the right side of the road.

### B. GAZE ANGLE

Under sharp bend conditions, changes in a driver's gaze angle reflect the distribution of attention in the driving process. The gaze angle reflects the change in a driver's main spatial

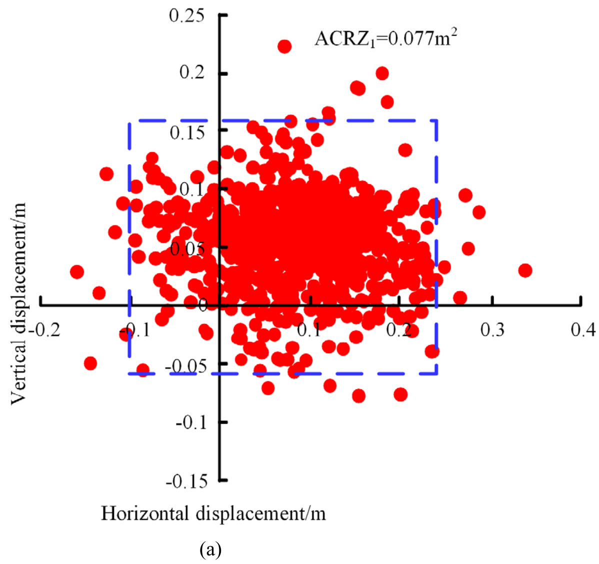


**FIGURE 3.** Fixation point position distribution in curved sections. (a) Right turn bends. (b) Left turn bends.

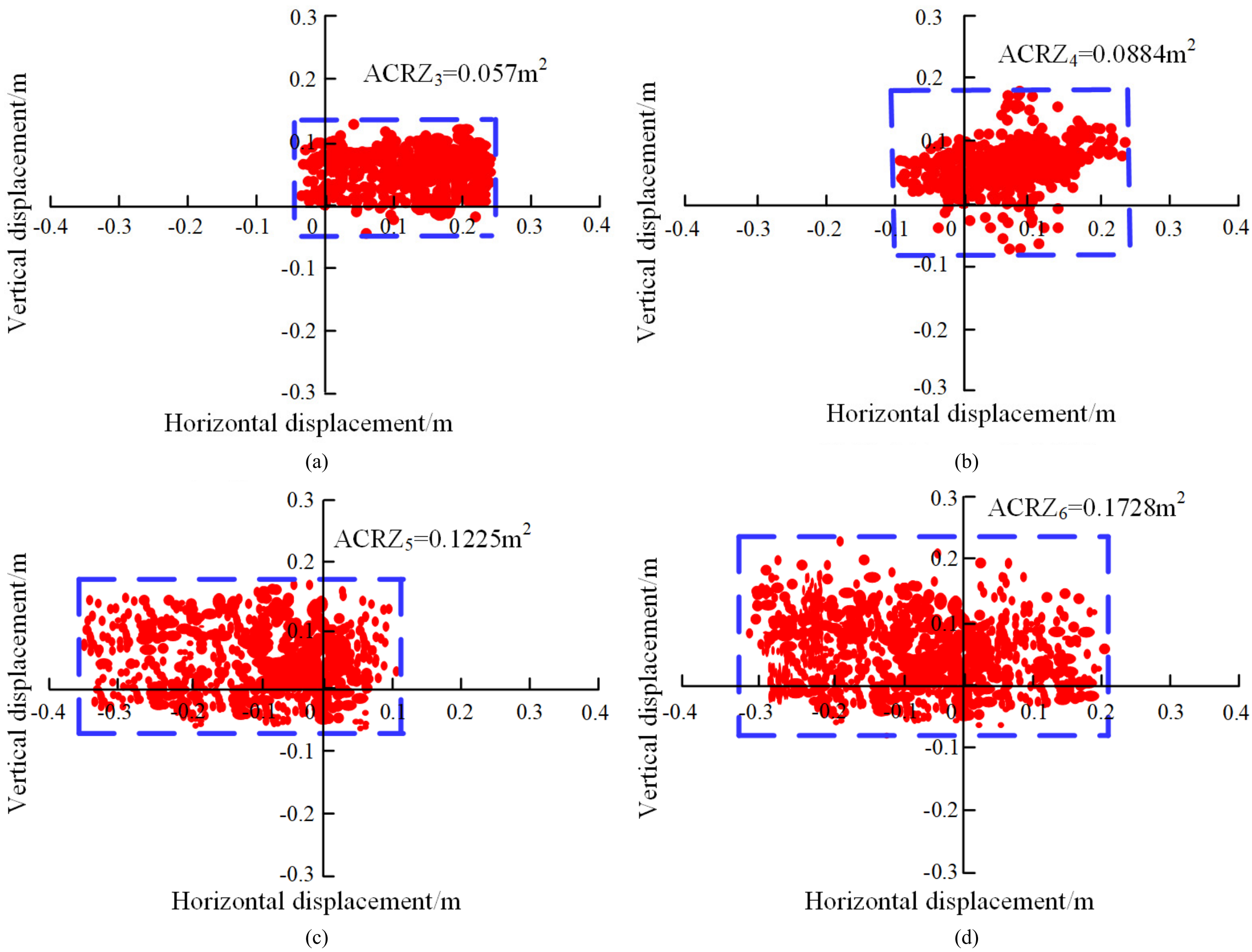


**FIGURE 4.** Distribution of fixation points in curved sections. (a) Right turn, R = 45.2 m (b) Right turn, R = 150.7 m. (c) Left turn, R = 33.5 m. (d) Left turn, R = 135.7 m.

attention over time, which can be divided into a horizontal gaze angle and a vertical gaze angle [25]. [26]. The horizontal gaze angle reflects the driver's horizontal gaze width and is taken as the absolute value of the angle between the line of sight and the vertical surface. The vertical gaze angle reflects the vertical gaze breadth of the driver's line of sight; a positive

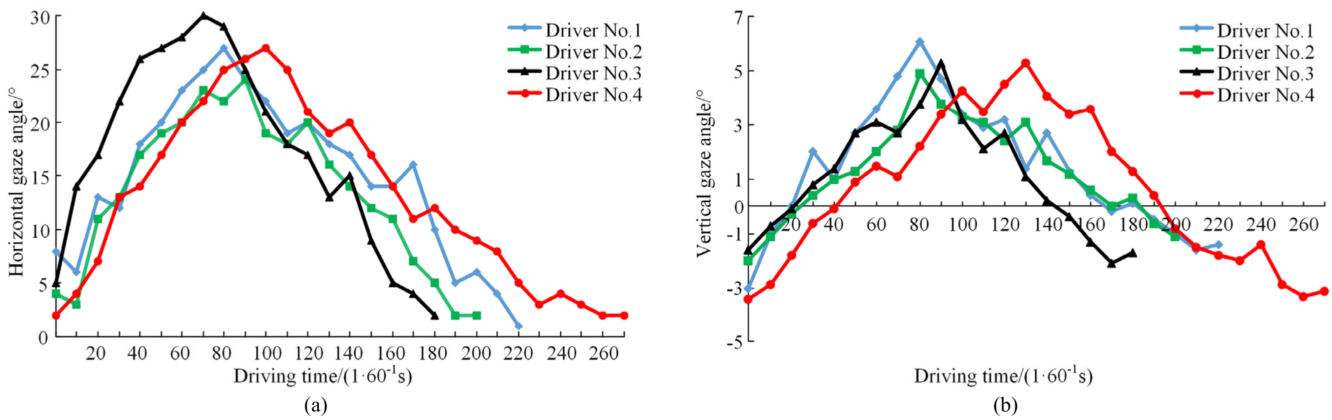


**FIGURE 5.** **Time-change curve of the gaze angle. (a) Horizonal gaze angle. (b) Vertical gaze angle.**

value indicates that the line of sight is focused on the road far ahead, and a negative value indicates that the line of sight is focused on the near side of the road. The statistics of all the sharp roads for No. 1-4 drivers' data are shown in Figure 5.

In the diagram, the abscissa represents the time series of the driving process, which means the time to turn, and the ordinate represents the driver's horizontal (or vertical) gaze angle. The data show that on sharp roads, the main range of a driver's horizontal gaze angle is 0-30°. The line of sight shifts from the front along with the curve. The horizontal gaze angle of the visual search increases gradually, and the horizontal gaze angle reaches a maximum at the end of clothoid curves during bends. Then, the line of sight gradually shifts back to the front with the end of the curve. The main range of a driver's vertical gaze angle is $-3$-6°, and the vertical gaze angle increases gradually to 6° along with the curve and then decreases gradually. This result indicates that the line of sight in the vertical direction is mainly concentrated on the nearby road surface before drivers enter curves, gradually shifts to the distant road surface and then gradually returns to the nearby road surface.

Comparing the time when the maximum absolute values of the horizontal and vertical gaze angles appear, it is found that the horizontal gaze angle reaches a maximum before the vertical gaze angle, indicating that at the end of the clothoid curves, drivers first perform a horizontal visual search before paying attention to the road ahead. Comparing the data of No.1-4 drivers, the difference is mainly reflected in the rate of change in the gaze angle. The rate of change in the gaze angle of drivers with high driving mileage is relatively stable, and the gaze angles of drivers 1 and 4, with less driving mileage, are more unstable.

### *C. SACCADE DURATION*

Saccade duration is the time a driver's attention shifts from one fixation point to the next. The more complex the road information, the greater the information density in a visual search area and the longer the saccade duration. This phenomenon indicates that saccade duration has a strong correlation with the complexity of traffic information to be processed [27], [28]. The statistics of all the sharp bends of the data of No.1-4drivers are shown in Figure 6.

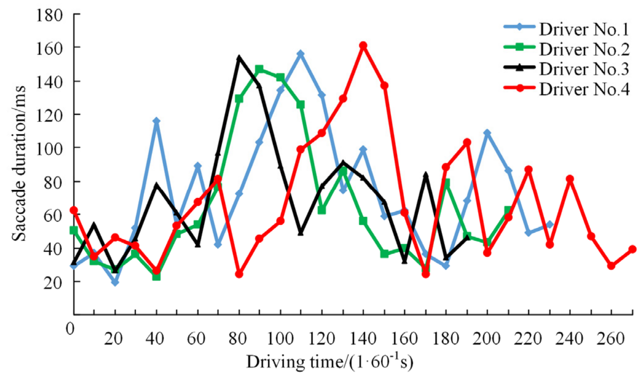


**FIGURE 6.** **Time-change curve of the saccade duration.**

It can be seen from the figure that saccade duration at the beginning of bends is lower, approximately 50 ms, indicating a short saccade period for drivers, a small density of visual searching information, an easy way to collect required surrounding information, and a light visual burden. In the middle of bends, the saccade duration fluctuates by a large margin and reaches a maximum value, indicating that drivers' scanning processes are prolonged, that visual search sensitivity is reduced, and that the efficiency of obtaining required surrounding information is also reduced. A maximum saccade time indicates that drivers have the largest visual burden in that time. After coming out of the turn, the saccade duration decreases to approximately 50 ms, which indicates that after turning, a driver's visual system changes from high burden and low sensitivity to low burden and high sensitivity. Compared Comparing the saccade duration of different drivers, it was found that drivers No. 1 and No. 4, both with less driving mileage, have a longer saccade duration; their ability to obtain effective information is relatively poor, and they have a much heavier visual burden.

### D. SACCADE AMPLITUDE

Saccade amplitude is the range of a driver's line of sight shifting from one fixation point to the next during a visual search, usually measured by an angle. In general, the saccade range can be used to describe a driver's attention depth. If the saccade amplitude is larger, the driver can obtain more information; however, the burden on the visual system is greater [29]. The statistics of all the sharp roads of the data from drivers No. 1-4 are shown in Figure 7.

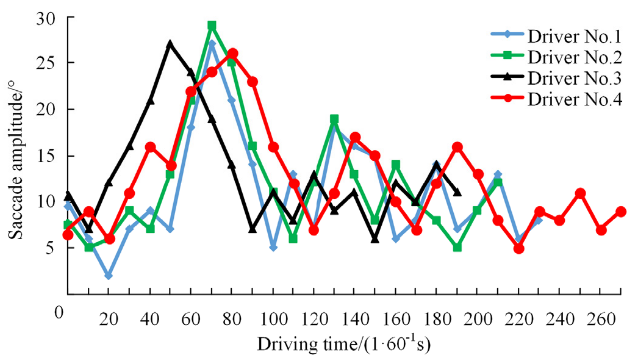


**FIGURE 7.** Time-change curve of the saccade amplitude.

In the process of entering and coming out of bends, the range of drivers' saccade amplitude is small, approximately 5-15°. In the middle of bends, the range of drivers' saccade amplitude reaches approximately 25°, which is the peak of drivers' saccade amplitude during each bend. This result shows that drivers have improved ability to obtain or process information to ensure driving safety when they pass bends on the road.

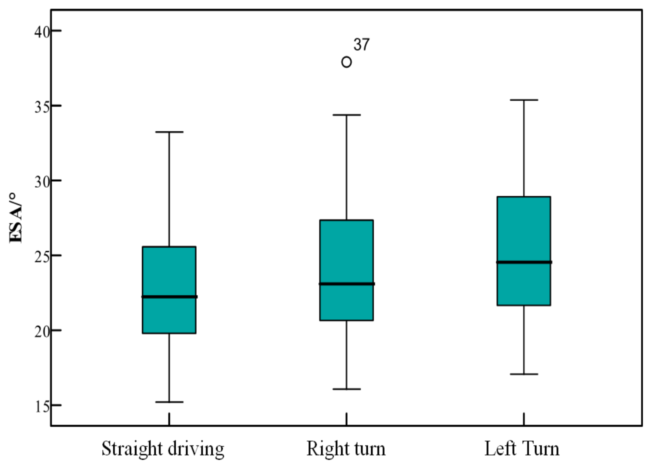


**FIGURE 8.** ESA distribution.

To comprehensively measure the basic characteristics of saccade behavior in the corresponding operating mode, the mean of all the saccade amplitudes, defined as the equilibrium saccade amplitude (ESA), is used. In this study, the size of the ESA of participants was measured in turning left, turning right, and straight driving modes, and the results are shown in Figure 8. Three quarters of the ESA values in the three modes were between 25° and 30°. Intuitively, the ESA, when driving straight, was slightly lower than when turning right and turning left, while the ESA when turning left was the highest. According to the homogeneity tests of a single-factor variance analysis, the results showed that the difference in ESA between the three modes was not significant; $p = 0.49 > 0.05$.

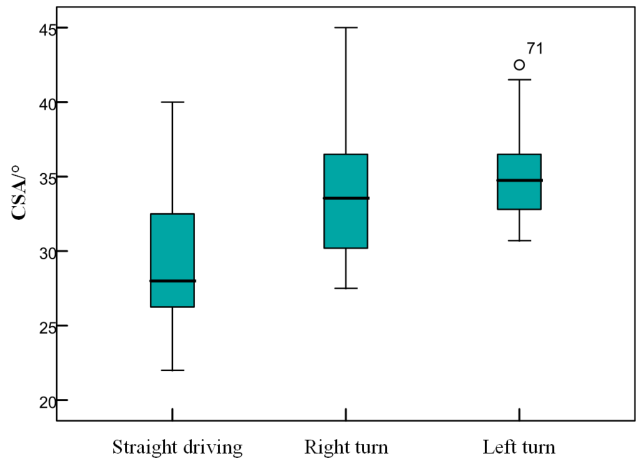


**FIGURE 9.** CSA distribution.

The maximum of all the saccade amplitudes was defined as the critical saccade amplitude (CSA), and the results for this measurement in the complete driving behavior mode are shown in Figure 9. Three quarters of the CSA values when driving straight were approximately 28°, while in the turning left and right operation modes, three quarters of the CSA values were between 30° and 35°. Intuitively, the CSA in the straight driving mode was lower than in the turning left and right modes. An independent-sample t-test was performed to compare the CSA in the straight driving and turning right groups, which indicated significant differences between the two groups; $p = 0 < 0.5$. Similarly, an independent-sample t-test was performed to compare the CSA in the turning right and left groups, indicating that the difference was not significant; $p = 0.75 > 0.5$. Therefore, the CSA when driving straight was significantly lower than that when turning right and left. To ensure driving safety, the fixation point of drivers will experience large-scale transfers from the inside curve (lane edge line, obstacles, etc.) to the outside curve (outside lane, other vehicles, etc.). Compared to driving straight, this type of visual search indicates that the driver expands their visual range to enhance visual searching and tracking of potentially dangerous targets in the turning process. Combined with the statistical results of ESA in Figure 8, this wide range of visual transitions is less frequent, thus ensuring that the quality and level of driver attention to the main task are not reduced while effectively extracting the boundary objects.

The results for the further statistical analysis of the relationship between the curve radius and CSA in the turning right and left modes are shown in Figure 10.

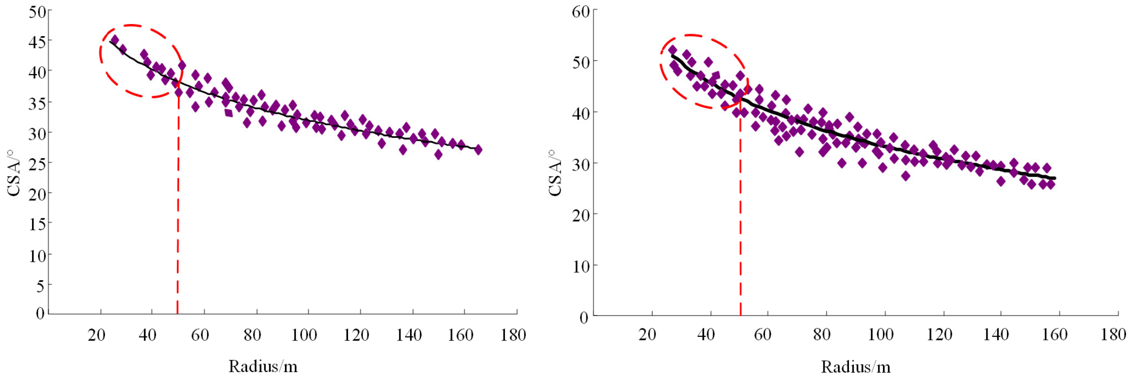


**FIGURE 10.** Scatter plots of the curve radius and CSA. (a) Right turn. (b) Left turn.

In the above picture, the data in the circles show the relationship for sharp turn curves. The CSA decreased as the curve radius increased, owing to the smaller curve radius, which implies a shorter stopping sight distance. To ensure driving safety, drivers need larger saccade amplitudes to ensure that the critical edge target is extracted and positioned. Evaluating the goodness-of-fit of the different functions, we found that the relationship between the curve radius ($R$) and the CSA value of right turn modes ($y1$), as well as the CSA value of left turn modes ($y2$), obey logarithmic function rules:

$$y_1 = -9.3651Ln(R) + 75.172 \tag{1}$$

$$y_2 = -13.61Ln(R) + 95.872 \tag{2}$$

### E. SACCADE VELOCITY

The saccade velocity can be used to describe the information processing speed of gaze behavior and drivers' visual search sensitivity from one target to the next [30]. The chart of eye saccade velocity for drivers No.1-4 in sharp road conditions is shown in Figure 11.

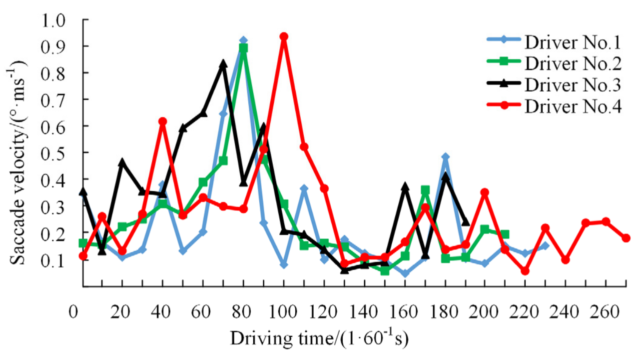


**FIGURE 11.** Time-change curve of the saccade velocity.

During sharp bends, the saccade velocity is obviously changed, and its range is 0-1$^\circ \cdot ms^{-1}$. At the beginning of sharp roads, saccade velocity increases and reaches a maximum at the end of the clothoid curves. At the end of bends, saccade velocity fluctuation decreases, eye burden gradually decreases, and drivers' tension is relieved.

### F. HEAD MOVEMENT CHARACTERISTICS

In the actual driving process, the visual search for external targets is the result of head and eye movement interactions. When two adjacent fixation points are close, even if the head is fixed, the driver only needs the appropriate saccade behavior to complete the visual transfer [31]. However, when two adjacent fixation points are separated by a longer distance, such as when transferring the fixation point from the front view to the side rearview mirror, then the visual search process cannot be completed by simply relying on the saccade behavior [32]. At this moment, first, the head of the driver needs to turn a certain angle; then, the eye displacement compensates for the movement of the head to complete the visual search behavior. In the three-dimensional coordinate system of the Smart Eye Pro 5.7, the head position is represented by three characteristic parameters: horizontal, vertical, and front and rear positions. The origin of the three-dimensional coordinate system is located at the center of the front two visual tracking cameras.

The mean value of the continuous head position of drivers when driving through the different curve sections was calculated, as shown in Figure 12. The curve radius and turning direction had little effect on the vertical as well as the front and rear positions of the head but had a larger effect on the horizontal head position. When the drivers turned right, the horizontal head position was between 0 m and 0.03 m, indicating that the head turned to the right; the smaller the curve radius is, the wider the horizontal movement of the head. Similarly, when the drivers turned left, the horizontal position of the head was between -0.035 m and 0 m, indicating that the head turned to the left at this time. Moreover, the level of horizontal head movement was inversely proportional to the curve radius. Comparing turning left, turning right, and driving straight, the horizontal head movement when turning left was the widest, followed by turning right and lastly driving straight.

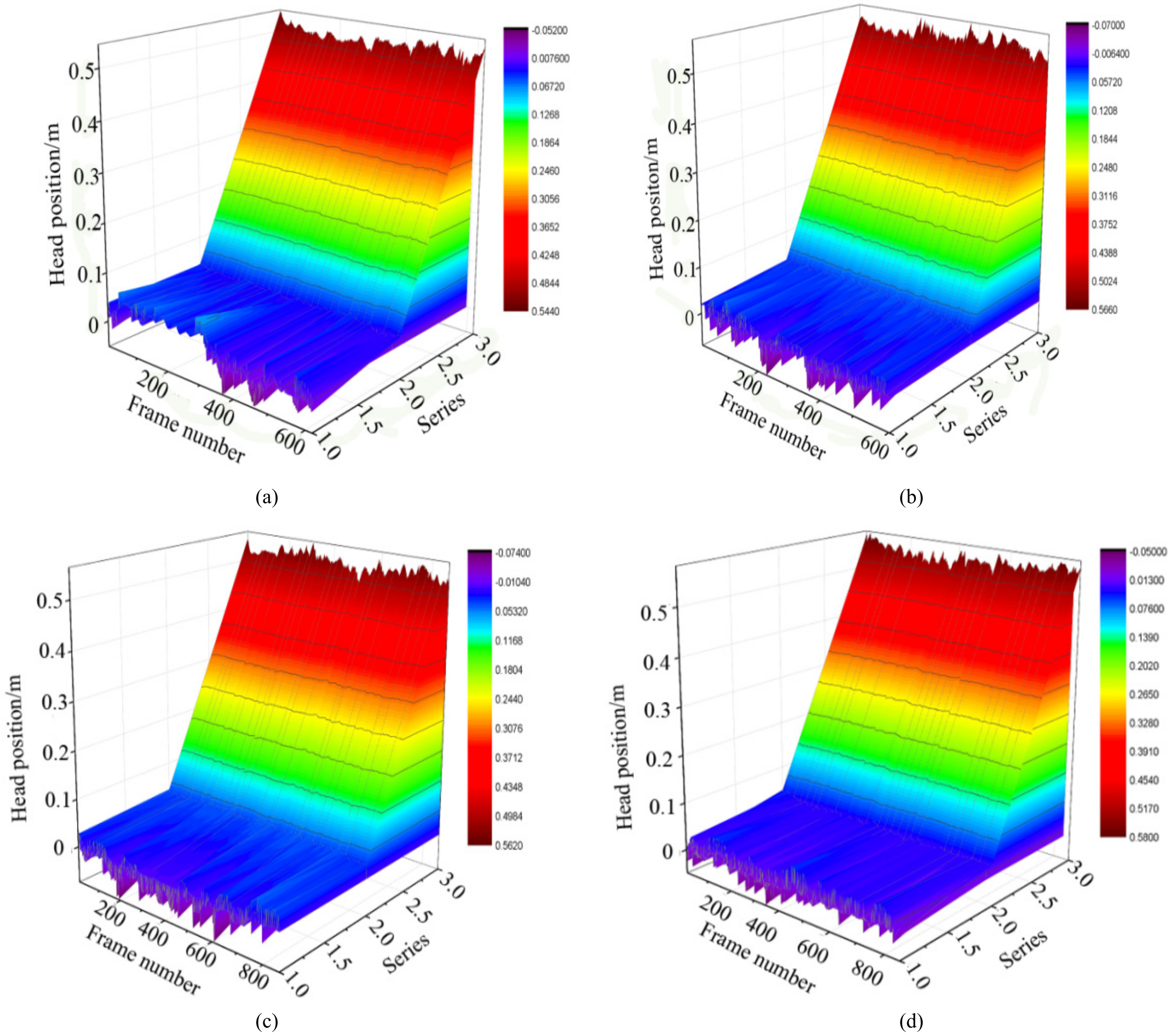


**FIGURE 12.** **Three-dimensional head position distribution in curves. (a) Right turn, R = 45.2 m. (b) Right turn, R = 150.7 m. (c) Left turn, R = 33.5 m. (d) Left turn, R = 135.7 m.**

## IV. EVALUATION METHOD OF DRIVING PROFICIENCY FOR POTENTIAL CONNECTED VEHICLES

### A. HYPOTHETICAL CONDITION

Proficiency evaluation is a complex system engineering problem, involving a large number of elements, and the coupling characteristics between the elements are highly unpredictable [33]. To simplify the problem, some assumptions are made as follows:

(1) There is a positive correlation between driving mileage and driving proficiency;

(2) Ignore the influence of abnormal driving behavior (e.g., distractions) on the visual characteristics data for a few sharp bends;

(3) Ignore the influence of a few data losses on the test results.

### B. PRINCIPAL COMPONENT ANALYSIS

Based on the idea of dimensionality reduction and the principle of minimum data information loss, a principal component analysis (PCA) is an optimal synthesis and simplification of a multivariable statistical method, which can convert multiple indexes into a few comprehensive indexes [34]. The principal components not related to each other are linear combinations of the original variables. The principal component analysis is used on the parameters of drivers' visual search characteristics to reduce the dimension of the original variables and then to evaluate each object systematically. A comprehensive evaluation model is also developed [35].

A comprehensive evaluation model based on the PCA needs to follow the following steps:

(1) Build an original matrix (if the data unit is different or if the order of magnitude is different, the data need to be standardized);

(2) Calculate the correlation matrix and its eigenvalues and obtain the contribution rate and the feature vector of the principal components;

(3) Obtain the comprehensive evaluation function by taking the eigenvalue of each principal component as the weight coefficient.

### C. DATA PROCESSING

In this study, a driving proficiency assessment model was built with left turn data as an example (if both left and right turn samples were analyzed, all the elements in the matrix would approach 0.) First, the collected data are filtered and eliminated. Then, all the bend data in the same index are simplified by the average value method, that is, the standardized visual search characteristics of each driver in all sharp bends are obtained. This paper stipulates that fixation point position (unit: meter) is $n_1$, horizontal gaze angle (unit: degree) is $n_2$, vertical gaze angle (unit: degree) is $n_3$, saccade duration (unit: millisecond) is $n_4$, saccade amplitude (unit: degrees) is $n_5$, and saccade velocity (unit: degrees per second) is $n_6$. Fixation point position is taken from the Euclidean distance from each point to the origin. Horizontal gaze angle and vertical gaze angle are unified for their absolute values to avoid the influence of their directionality [36], [37].

After data processing is completed, the original matrix built from the relevant data of 20 drivers is $X_1$, as shown at the bottom of this page.

Each row represents a driver's 6 index values, totaling 20 rows, and each column represents the data values of different drivers with the same eye movement characteristics. The first column of data is fixation point position, the second column of data is horizontal gaze angle, the third column of data is vertical gaze angle, the fourth column of data is saccade duration, the fifth column of data is saccade amplitude, and the sixth column of data is saccade velocity.

Due to the large differences between each indicator in their units and the orders of magnitude, it is necessary to standardize the matrix to reduce the differences of each index in a comprehensive analysis [38], [39]. The correlation matrix and its eigenvalue as well as the contribution rate and its feature vector of each principal component can be obtained by using Matlab software, as seen in Table 1 below.

**TABLE 1. Principal component eigenvalues and contribution rates.**

| Principal components | Eigenvalues | Contribution rate | Cumulative contribution rate |
|---|---|---|---|
| F1 | 1.98 | 0.33 | 0.33 |
| F2 | 1.4727 | 0.2454 | 0.5754 |
| F3 | 1.21844 | 0.2031 | 0.7785 |
| F4 | 0.778 | 0.1297 | 0.9082 |
| F5 | 0.3959 | 0.066 | 0.9742 |
| F6 | 0.1551 | 0.0258 | 1 |

Finally, with reference to the cumulative contribution rate of the principal component, principal component selection is based on cumulative contribution rates above 90%. It can be seen from the above table that the cumulative contribution rate of the max four principal components is 0.9082. The max four principal components are selected as new indexes for comprehensive evaluation, as follows:

$$F1 = -0.0523n'_1 - 0.3158n'_2 + 0.7614n'_3 - 0.248n'_4 + 0.4728n'_5 - 0.1812n'_6 \quad (3)$$

$$F2 = -0.5189n'_1 + 0.1236n'_2 + 0.3387n'_3 + 0.5825n'_4 - 0.0188n'_5{+}0.511n'_6 \quad (4)$$

$$F3 = 0.4656n'_1 - 0.2664n'_2 - 0.2073n'_3 + 0.6244n'_4 + 0.5283n'_5 - 0.0.175n'_6 \quad (5)$$

$$F4 = -0.2056n'_1 + 0.6757n'_2 - 0.2012n'_3 - 0.1793n'_4 - 0.6546n'_5 - 0.0104n'_6 \quad (6)$$

By the analysis of the load vectors of each principal component, the vertical fixing angle $n_3$ and the saccade

$$X_1 = \begin{bmatrix} 0.2143 & 29.09 & 1.7349 & 73.5869 & 27.1269 & 263.4182 \\ 0.2956 & 27.1498 & 1.976 & 61.9048 & 29.7868 & 317.1724 \\ 0.2905 & 35.1462 & 1.0755 & 73.7006 & 21.6793 & 301.328 \\ 0.2167 & 29.8633 & 2.7703 & 69.4854 & 24.899 & 295.1774 \\ 0.2648 & 33.6122 & 1.8266 & 61.4631 & 20.2867 & 378.567 \\ 0.2018 & 24.3506 & 2.5924 & 64.1775 & 28.8651 & 305.1584 \\ 0.1869 & 25.0262 & 1.1974 & 68.2032 & 22.3993 & 371.7137 \\ 0.1985 & 32.764 & 1.5237 & 74.3626 & 21.8292 & 316.6561 \\ 0.2196 & 30.0943 & 1.6707 & 74.4733 & 25.7672 & 349.771 \\ 0.2945 & 30.9423 & 2.3595 & 62.3642 & 28.0549 & 272.3821 \\ 0.3162 & 26.8474 & 1.2731 & 74.5589 & 26.9875 & 306.1622 \\ 0.1854 & 29.5062 & 2.4425 & 74.3575 & 21.9781 & 300.4838 \\ 0.3166 & 35.5571 & 1.2135 & 67.2806 & 20.3054 & 319.3111 \\ 0.2744 & 30.5617 & 2.3075 & 72.0042 & 27.4407 & 248.6435 \\ 0.2448 & 30.2536 & 1.9883 & 62.1283 & 25.0002 & 232.7656 \\ 0.3082 & 26.7791 & 2.5581 & 66.3264 & 24.7992 & 344.3642 \\ 0.2594 & 29.8668 & 1.4301 & 73.736 & 29.0472 & 214.3337 \\ 0.1942 & 31.4887 & 1.8074 & 71.8831 & 26.0987 & 291.9375 \\ 0.2073 & 32.1496 & 1.7818 & 74.3924 & 26.1767 & 257.654 \\ 0.2381 & 28.7462 & 1.6683 & 698361 & 28.5944 & 226.6597 \end{bmatrix}$$

**TABLE 2. Comprehensive score for drivers' eye movements.**

| Number | Gender | Age | Driving years | Driving mileage/ $10^4$km | Eye movement comprehensive score |
|---|---|---|---|---|---|
| 1 | male | 45 | 18 | 10 | -0.2758 |
| 2 | male | 40 | 22 | 80 | 0.8707 |
| 3 | male | 42 | 16 | 40 | 0.2601 |
| 4 | female | 34 | 6 | 10 | -0.2248 |
| 5 | male | 44 | 12 | 50 | 0.4334 |
| 6 | male | 32 | 10 | 9 | -0.6220 |
| 7 | male | 31 | 5 | 7 | -0.8552 |
| 8 | male | 26 | 3 | 7 | -0.5674 |
| 9 | female | 33 | 5 | 5 | -1.2002 |
| 10 | male | 36 | 8 | 10 | -0.0090 |
| 11 | male | 48 | 25 | 100 | 1.0033 |
| 12 | female | 32 | 4 | 3 | -1.2871 |
| 13 | male | 33 | 12 | 50 | 0.4928 |
| 14 | male | 45 | 8 | 35 | 0.1895 |
| 15 | male | 32 | 4 | 15 | 0.0776 |
| 16 | male | 36 | 10 | 60 | 0.5912 |
| 17 | female | 37 | 5 | 10 | -0.4641 |
| 18 | male | 43 | 20 | 40 | 0.3982 |
| 19 | male | 38 | 14 | 40 | 0.4067 |
| 20 | male | 38 | 13 | 60 | 0.7821 |

amplitude $n_5$ have a large influence on the common factor $F1$, which can be used to describe the vertical visual search speed to evaluate driving proficiency. The fixation point position $n_1$ and the saccade duration $n_4$ have a large influence on the common factor $F2$, which can be used to describe the changeable fixation range to evaluate driving proficiency. The saccade duration $n_4$ and the saccade amplitude $n_5$ have a large influence on the common factor $F3$, which can be used to describe the saccade behavior to evaluate driving proficiency. The horizontal gaze angle $n_2$ and the saccade amplitude $n_5$ have a large influence on the common factor $F4$, which can be used to describe the horizontal visual search speed to evaluate driving proficiency.

Taking the eigenvalue of each principal component as the weight, the following formula is obtained by weighting each principal component:

$$Score = 0.3634F1 + 0.2702F2 + 0.2236F3 + 0.1428F4 \tag{7}$$

Using the above formula, a comprehensive eye movement score for 20 drivers can be obtained, as shown in Table 2.

## V. DISCUSSION AND CONCLUSION

Twenty drivers' data and information in the above table are reordered according to their eye movement comprehensive score, and the relationships of eye movement comprehensive scores with driving mileage are shown in Figure 13 below.

The figure shows that with an increase in driving mileage, eye movement comprehensive score increases gradually, that is, driving mileage and eye movement comprehensive score show a positive correlation. Therefore, by using these six eye movement parameters, driving proficiency can be accurately identified. In addition, the eye movement comprehensive score is also affected by other factors. For example, the driving mileage of driver No. 8 is less than that of driver No. 6, but he is younger and has a higher driving frequency.

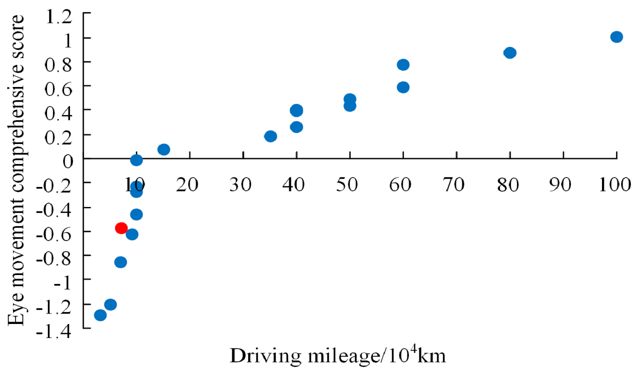


**FIGURE 13. Relationship between driving mileage and eye movement comprehensive score.**

Therefore, he is judged to be relatively skillful, owing to his sensitive eye movements, which makes his eye movement comprehensive score higher than driver No. 6. For drivers with the same driving mileage, the eye movement comprehensive score is mainly influenced by age. Generally, younger drivers have more flexible visual search ability and higher comprehensive scores. We used independent-samples T test to verify if the gender has remarkable effect on eye movement comprehensive score, $p = 0.004 < 0.05$, so we may conclude that male drivers tend to get significantly higher visual comprehensive scores than female drivers.

With the method proposed in our research, we could draw the conclusion that which drivers are more skilled than others in a particular group. However, we cannot obtain a discriminant standard to judge whether or not a driver is skilled, that is, the skill level we achieved in this research is relative rather than absolute value. Moreover, based upon the designed field experiment under complex driving conditions, the parameter matrix we built in this paper could be used to evaluate the visual search abilities of connected or autonomous vehicles travelling on mountain roads.

Based on related research results and analyses of six eye movement characteristic parameters, the results are as follows:

(1) Visual gaze behavior: on right turn bends, the distribution of the driver's fixation points in the horizontal direction is −0.1-0.25 m, and on left turn bends is −0.35-0.18 m, indicating that visual search is mainly focused on information from the inner side of the curve. The main range of horizontal gaze angle is 0-30°, and the main range of vertical gaze angle is −3-6°. Drivers give priority to the horizontal direction of the visual search.

(2) When turning right, the larger the curve radius, the more diffuse the fixation point distribution ($ACRZ_3 = 0.057\ m^2$, $ACRZ_4 = 0.0884\ m^2$), which indicates that the driver is in a relatively comfortable driving state. With a small curve radius, the fixation points of drivers are more displaced towards the right. Similar to the right turn, the larger the curve radius, the more diffuse the fixation point distribution ($ACRZ_5 = 0.1225\ m^2$, $ACRZ_6 = 0.1728\ m^2$). When turning left in curves with a large radius, drivers will focus more visual attention on the right of the road.

(3) Visual saccade behavior: in the course of sharp turning, the range of saccade velocity is 0-1° $\cdot$ $ms^{-1}$, the saccade duration can be up to 160 ms in unit time (0.33 s), and the saccade amplitude also increases from 5° to 25°. Furthermore, the CSA was inversely proportional to the curve radius.

(4) There is a positive correlation between eye movement comprehensive score and driving mileage; thus, the driving proficiency can be evaluated with the comprehensive score of six eye movement index parameters. Although driving proficiency depends mainly on driving mileage, it is also affected by other factors, such as age and driving frequency [40].

There are still a few aspects of our work that need to be improved in future research. In this study, the model is built according to data for sharp turn bends. To improve the accuracy of the results, more different types of road tests should be launched, and visual behavior big data should be recorded and applied. In addition, in this study, visual search characteristics are the key elements, but there are actually many other different factors that have large influences on driving proficiency. Thus, a future study will focus on building evaluation models not only based on eye movement characteristics, and then discriminate drivers who could be proficient enough to take the job as long distance bus drivers.

## REFERENCES


[1] G. Cardona and N. Quevedo, "Blinking and driving: The influence of saccades and cognitive workload," *Current Eye Res.*, vol. 39, no. 3, pp. 239–244, Mar. 2014.

[2] J. B. Hu, W. L. Wang, and S. R. Zhang, "Safety analysis of car drivers fixation characteristics freeways," *J. Southwest Jiaotong Univ.*, vol. 47, no. 2, pp. 299–305, Apr. 2012.

[3] X. Huang, Y. Liu, J. Duan, and H. M. Zhang, "The assessment of traffic accident risk based on grey relational analysis and fuzzy comprehensive evaluation method," *Math. Pract. Theory*, vol. 47, no. 7, pp. 208–215, Apr. 2017.

[4] M. Muñoz-Organero and V. Corcoba-Magaña, "Predicting upcoming values of stress while driving," *IEEE Trans. Intell. Transp. Syst.*, vol. 18, no. 7, pp. 1802–1811, Nov. 2017.

[5] A. Sundström, "The validity of self-reported driver competence: Relations between measures of perceived driver competence and actual driving skill," *Transp. Res. F, Traffic Psychol. Behav.*, vol. 14, no. 2, pp. 155–163, Mar. 2011.

[6] H. Liu, T. Taniguchi, Y. Tanaka, K. Takenaka, and T. Bando, "Visualization of driving behavior based on hidden feature extraction by using deep learning," *IEEE Trans. Intell. Transp. Syst.*, vol. 18, no. 9, pp. 2477–2489, Sep. 2017.

[7] A. K. Mackenzie and J. M. Harris, "A link between attentional function, effective eye movements, and driving ability," *J. Exp. Psychol.-Hum. Perception Perform.*, vol. 43, no. 2, pp. 381–394, Feb. 2017.

[8] M. Jäger, N. Gruber, R. Müri, U. P. Mosimann, and T. Nef, "Manipulations to reduce simulator-related transient adverse health effects during simulated driving," *Med. Biol. Eng. Comput.*, vol. 52, no. 7, pp. 601–610, Jun. 2014.

[9] C. E. J. Key, A. P. Morris, and N. J. Mansfield, "Situation awareness: Its proficiency amongst older and younger drivers, and its usefulness for perceiving hazards," *Transp. Res. F, Traffic Psychol. Behav.*, vol. 40, pp. 156–168, Jul. 2017.

[10] A. Gugliotta *et al.*, "Are situation awareness and decision-making in driving totally conscious processes? Results of a hazard prediction task," *Transp. Res. F, Traffic Psychol. Behav.*, vol. 44, pp. 168–179, Jan. 2017.

[11] S. Kaplan, M. A. Guvensan, A. G. Yavuz, and Y. Karalurt, "Driver behavior analysis for safe driving: A survey," *IEEE Trans. Intell. Transp. Syst.*, vol. 16, no. 6, pp. 3017–3032, Dec. 2015.

[12] D. Crundall and G. Undrewood, "Effects of experience and processing demands on visual information acquisition in drivers," *Ergonomics*, vol. 41, no. 4, pp. 448–458, Nov. 1998.

[13] S. O'Regan, S. Faul, and W. Marnane, "Automatic detection of EEG artefacts arising from head movements using EEG and gyroscope signals," *Med. Eng. Phys.*, vol. 35, no. 7, pp. 867–874, Jul. 2013.

[14] L. M. Martinussen, M. Møller, and C. G. Prato, "Accuracy of young male drivers' self-assessments of driving skill," *Transp. Res. F, Traffic Psychol. Behav.*, vol. 46, pp. 228–325, Apr. 2017.

[15] Y. S. Guo, W. Yuan, R. Fu, and C. L. Xue, "Evaluation method of driving proficiency based on fixation transition mode," *J. Traffic Transp. Eng.*, vol. 14, no. 4, pp. 98–104, Aug. 2014.

[16] L. Zhao and L. Y. Xu, "Research on visual search patterns of new and old drivers in mountainous rural roads," *J. Wuhan Univ. Technol. (Transp. Sci. Eng.)*, vol. 41, no. 2, pp. 294–297, Apr. 2017.

[17] G. Underwood, P. Chapman, N. Brocklehurst, J. Underwood, and D. Crundall, "Visual attention while driving: Sequences of eye fixations made by experienced and novice drivers," *Ergonomics*, vol. 46, pp. 629–646, Jun. 2003.

[18] G. Underwood, "Visual attention and the transition from novice to advanced driver," *Ergonomics*, vol. 50, no. 8, pp. 1235–1249, Aug. 2007.

[19] C. Ahlstrom *et al.*, "Fit-for-duty test for estimation of drivers' sleepiness level: Eye movements improve the sleep/wake predictor," *Transp. Res. C, Emerg. Technol.*, vol. 26, pp. 20–32, Jan. 2013.

[20] N. Arbabzadeh and M. Jafari, "A data-driven approach for driving safety risk prediction using driver behavior and roadway information data," *IEEE Trans. Intell. Transp. Syst.*, vol. 19, no. 2, pp. 446–460, Jun. 2017.

[21] S. J. Wang, C. Zhang, L. Jin, D. J. Shao, and X. N. Ma, "Auxiliary decision-making method on risky sharp turn section in mountain area based on fuzzy comprehensive evaluation," *China J. Highway Transp.*, vol. 28, no. 12, pp. 120–127, Apr. 2015.

[22] F. Kubo, B. Hablitzel, M. D. Maschio, W. Driever, H. Baier, and A. B. Arrenberg, "Functional architecture of an optic flow-responsive area that drives horizontal eye movements in Zebrafish," *Neuron*, vol. 81, no. 6, pp. 1344–1359, Mar. 2014.

[23] L. Yekhshatyan and J. D. Lee, "Changes in the correlation between eye and steering movements indicate driver distraction," *IEEE Trans. Intell. Transp. Syst.*, vol. 14, no. 1, pp. 136–145, Mar. 2013.

[24] G. L. Yan, H. J. Tian, and X. F. Zhang, "Eye movement study of driving behavior," *Psychol. Sci.*, vol. 28, no. 5, pp. 1211–1212, Sep. 2005.

[25] C. R. Latimer, "Eye-movement data: Cumulative fixation time and cluster analysis," *Behav. Res. Methods, Instrum., Comput.*, vol. 20, no. 5, pp. 437–470, Sep. 1988.

[26] A. Borowsky, T. Oron-Gilad, and Y. Parmet, "Age and skill differences in classifying hazardous traffic scenes," *Transp. Res. F, Traffic Psychol. Behav.*, vol. 12, no. 4, pp. 277–287, Jul. 2009.

[27] Y. Cheng and L. Gao, "Analysis of glance movements of driver in act of U-turn urban expressway," *China Saf. Sci. J.*, vol. 25, no. 8, pp. 87–92, Aug. 2015.

[28] J. M. Cooper, N. Medeiros-Ward, and D. L. Strayer, "The impact of eye movements and cognitive workload on lateral position variability in driving," *Hum. Factors*, vol. 55, no. 5, pp. 1001–1114, Oct. 2013.

[29] Y. S. Guo, Y. Ma, R. Fu, N. Meng, and W. Yuan, "Influence of driving experience on gazing behavior characteristic for car driver," *J. Traffic Transp. Eng.*, vol. 12, no. 5, pp. 91–99, Oct. 2012.

[30] J. L. Orquin and S. M. Loose, "Attention and choice: A review on eye movements in decision making," *Acta Psychol.*, vol. 144, no. 1, pp. 190–206, Sep. 2013.

[31] M. Sağlam, N. Lehnen, and S. Glasauer, "Optimal control of natural eye-head movements minimizes the impact of noise," *J. Neurosci.*, vol. 31, no. 45, pp. 16185–16193, Nov. 2011.

[32] C. T. Bonnet and P. Despretz, "Large lateral head movements and postural control," *Hum. Movement Sci.*, vol. 31, no. 6, pp. 1541–1551, Dec. 2012.

[33] J. Peng, Y. Guo, R. Fu, W. Yuan, and C. Wang, "Multi-parameter prediction of drivers' lane-changing behaviour with neural network model," *Appl. Ergonom.*, vol. 50, pp. 207–217, Sep. 2015.

[34] J. S. Peng, R. Fu, and Y. M. Shao, "Systematic analysis of road traffic safety," *J. Chang'an Univ. (Natural Sci. Ed.)*, vol. 30, no. 6, pp. 72–75, Nov. 2010.

[35] F. Wang, F. Chen, F. J. Ni, R. R. Ge, and Y. Y. Cheng, "Correlation analysis between highway horizontal alignment and driversâĂŹ visual search behavior," *J. Southeast Univ. (Natural Sci. Ed.)*, vol. 39, no. 5, pp. 1070–1074, Sep. 2009.

[36] J. Li, G. Deng, C. Luo, Q. Lin, Q. Yan, and Z. Ming, "A hybrid path planning method in unmanned air/ground vehicle (UAV/UGV) cooperative systems," *IEEE Trans. Veh. Technol.*, vol. 65, no. 12, pp. 9585–9596, Dec. 2016.

[37] J.-Q. Li, F. R. Yu, G. Deng, C. Luo, Z. Ming, and Q. Yan, "Industrial Internet: A survey on the enabling technologies, applications, and challenges," *IEEE Commun. Surveys Tuts.*, vol. 19, no. 3, pp. 1504–1526, 3rd Quart., 2017.

[38] Y. G. Sun, H. Y. Qiang, J. Q. Xu, and D. S. Dong, "The nonlinear dynamics and anti-sway tracking control for offshore container crane on a mobile harbor," *J. Marine Sci. Technol.-Taiwan*, vol. 25, no. 6, pp. 656–665, Dec. 2017.

[39] P. Xiao, J. Wu, M. Sellathurai, T. Ratnarajah, and E. G. Strom, "Iterative multiuser detection and decoding for DS-CDMA system with space-time linear dispersion," *IEEE Trans. Veh. Technol.*, vol. 58, no. 5, pp. 2343–2353, Jun. 2009.

[40] J. Peng and Y. Shao, "Intelligent method for identifying driving risk based on V2V multisource big data," *Complexity*, vol. 2018, May 2018, Art. no. 1801273, doi: 10.1155/2018/1801273.


**JINSHUAN PENG** received the M.S. degree in vehicle operation engineering from Chongqing Jiaotong University in 2009 and the Ph.D. degree in vehicle operation engineering from Chang'an University in 2012. He is currently a Professor of transportation with Chongqing Jiaotong University. His current research interests include driving behavior and road traffic safety.

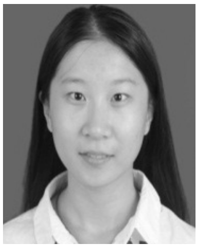

**CHENWEI WANG** was born in Anyang, Henan, China, in 1994. She received the B.S. degree from Chongqing Jiaotong University, Chongqing, in 2017, where she is currently pursuing the M.S. degree. Her research interests include driving behavior analysis and road safety system engineering.

**YIMING SHAO** received the Ph.D. degree in vehicle operation engineering from Chang'an University in 2006. He is currently a famous Professor of transportation with Chongqing Jiaotong University. His current research interests include driving behavior and road traffic safety.

**JIN XU** received the Ph.D. degree in traffic engineering from Chongqing Jiaotong University. He is currently a Professor of transportation with Chongqing Jiaotong University. His current research interests include driving behavior and road traffic safety.